



Article

Molecular Characterization of the Response to Conventional Chemotherapeutics in Pro-B-ALL Cell Lines in Terms of Tumor Relapse

Yvonne Saara Gladbach ^{1,2,3,†}, Lisa-Madeleine Sklarz ^{4,†}, Catrin Roof ⁴, Julia Beck ⁵, Ekkehard Schütz ⁵, Georg Fuellen ¹, Christian Junghanss ⁴, Hugo Murua Escobar ^{4,6}  and Mohamed Hamed ^{1,*} 

- ¹ Institute for Biostatistics and Informatics in Medicine and Ageing Research (IBIMA), Rostock University Medical Center, 18057 Rostock, Germany; y.s.gladbach@hotmail.de (Y.S.G.); fuellen@uni-rostock.de (G.F.)
² Faculty of Biosciences, Heidelberg University, 69120 Heidelberg, Germany
³ Division of Applied Bioinformatics, German Cancer Research Center (DKFZ), 69120 Heidelberg, Germany
⁴ Clinic III—Hematology, Oncology, Palliative Medicine, Center for Internal Medicine, Rostock University Medical Center, 18057 Rostock, Germany; lisa-madeleine.sklarz@uni-rostock.de (L.-M.S.); catrin.roof@gmail.com (C.R.); christian.junghanss@med.uni-rostock.de (C.J.); hugo.murua.escobar@med.uni-rostock.de (H.M.E.)
⁵ Chronix Biomedical GmbH, 37073 Göttingen, Germany; jbeck@chronixbiomedical.de (J.B.); esc@chronixbiomedical.de (E.S.)
⁶ Comprehensive Cancer Center Mecklenburg-Vorpommern (CCC-MV), Campus Rostock, Rostock University Medical Center, 18057 Rostock, Germany
* Correspondence: mohamed.hamed@uni-rostock.de
† These authors contributed equally to this work.



Citation: Gladbach, Y.S.; Sklarz, L.-M.; Roof, C.; Beck, J.; Schütz, E.; Fuellen, G.; Junghanss, C.; Murua Escobar, H.; Hamed, M. Molecular Characterization of the Response to Conventional Chemotherapeutics in Pro-B-ALL Cell Lines in Terms of Tumor Relapse. *Genes* **2022**, *13*, 1240. <https://doi.org/10.3390/genes13071240>

Academic Editor: Gael Roue

Received: 26 May 2022

Accepted: 29 June 2022

Published: 14 July 2022

Publisher's Note: MDPI stays neutral with regard to jurisdictional claims in published maps and institutional affiliations.



Copyright: © 2022 by the authors. Licensee MDPI, Basel, Switzerland. This article is an open access article distributed under the terms and conditions of the Creative Commons Attribution (CC BY) license (<https://creativecommons.org/licenses/by/4.0/>).

Abstract: Little is known about optimally applying chemotherapeutic agents in a specific temporal sequence to rapidly reduce the tumor load and to improve therapeutic efficacy. The clinical optimization of drug efficacy while reducing side effects is still restricted due to an incomplete understanding of the mode of action and related tumor relapse mechanisms on the molecular level. The molecular characterization of transcriptomic drug signatures can help to identify the affected pathways, downstream regulated genes and regulatory interactions related to tumor relapse in response to drug application. We tried to outline the dynamic regulatory reprogramming leading to tumor relapse in relapsed MLL-rearranged pro-B-cell acute lymphoblastic leukemia (B-ALL) cells in response to two first-line treatments: dexamethasone (Dexa) and cytarabine (AraC). We performed an integrative molecular analysis of whole transcriptome profiles of each treatment, specifically considering public knowledge of miRNA regulation via a network-based approach to unravel key driver genes and miRNAs that may control the relapse mechanisms accompanying each treatment. Our results gave hints to the crucial regulatory roles of genes leading to Dexa-resistance and related miRNAs linked to chemosensitivity. These genes and miRNAs should be further investigated in preclinical models to obtain more hints about relapse processes.

Keywords: drug response; tumor relapse; acute lymphoblastic leukemia; cytostatics; cytarabine; dexamethasone

1. Introduction

Acute lymphoblastic leukemia (ALL) is a heterogeneous disease characterized by a clonal proliferation of lymphoid precursor cells of the bone marrow, most commonly B-cells (B-ALL) [1–4]. Children with ALL have a long-term survival of 80% [4,5], whereas adults show a <30% disease-free survival [6]. Besides age, genetic rearrangements such as translocations indicate higher chances for relapse and a poor overall survival rate. Patients harboring a rearrangement of the histone-lysine N-methyltransferase 2A (KMT2A) gene on chromosome 11 have a poorer prognosis compared to patients without [7–9] due to resistance to treatment [10].

Different chemotherapeutic agents were used to reduce the amount of leukemic cells and to amend clinical protocols of radiation, immunotherapy and transplantation. The clinical protocols depend on factors such as the vital state of the patient, risk stratification of the different leukemic subtypes, and response to therapy. Several agents are currently applied using different protocols and show remarkable effectivity in the clinics. Nevertheless, it is possible that patients are affected by remaining malignant cells caused by treatment resistance leading finally to a relapse [7,11–13].

The treatment regimens of adult ALL were adapted from childhood ALL [14] and chronic lymphoblastic leukemia (CLL) protocols [11]. These therapeutic protocols suggested the application of several cytostatic agents, including glucocorticoids (GCs) such as dexamethasone (Dexa), as well as cytarabine (AraC) [1,15,16]. The GC Dexa is a long-established agent in the current treatment regimen [17–19] and binds to specific cytoplasmic GC receptors. It mediates the inflammatory response by inhibiting leukocyte infiltration at the inflammation site [19], acts as an anti-inflammatory drug, is used in cancer therapies and has a pro-apoptotic effect on malignancies with lymphoproliferative disorders. AraC is a nucleoside analog and it is incorporated into the DNA to directly inhibit the DNA polymerase, affecting DNA synthesis in the S phase of the cell cycle [20]. This makes AraC a main agent for the induction and extra-compartment therapy [21], either as a monotherapy or in combination with targeted agents [16]. While Dexa and AraC are highly effective in B-ALL treatment, their efficacy is still limited by severe adverse effects and a high relapse incidence [7]. For instance, 20% of B-ALL patients who are treated by GCs relapse and die from the disease [20], and survivors often suffer lifelong adverse effects [22,23]. Often, therapeutic success is limited, caused by remaining minimal residual disease after transplantation and/or chemotherapy [13] and the development of drug resistance [7]. Therefore, understanding relapse mechanisms is important for the choice of the clinical protocols and for developing superior treatment protocols.

The tumor escape mechanisms are not well-characterized yet in B-ALL [24]. Useful insights can be gained by understanding the mode of action of therapeutic agents on pro-B-ALL cell lines such as SEM and RS4;11. RS4;11 is a good model to investigate adult relapsed forms of KMT2A-rearranged pro-B-ALL, while SEM is suitable for the study of the childhood type [25]. Apart from their KMT2A-rearrangement, both cell lines were chosen specifically because of their isolation after relapse and their respective resistance to AraC (RS4;11) or Dexa (SEM).

Therefore, both cell lines were previously used to elucidate relapse-specific gene expression signatures [26]. These cells were previously incubated with AraC, as well as other nucleotide analogs, such as decitabine, zebularine, gemcitabine, and floxuridine [27,28]. Other studies incubated these cells with the GCs Dexa and prednisolone [29] to study the molecular mechanisms of GC-resistance [30,31].

To better understand the regulatory reprogramming associated with tumor relapse in response to Dexa and AraC, we here report a detailed investigation of the dynamic molecular responses of RS4;11 and SEM to both treatments. Cell-biological assays analyzing cell proliferation and metabolism revealed resistance mechanisms for AraC in RS4;11 and Dexa in SEM, which was as expected. We jointly analyzed the whole transcriptome profiles describing the effects of the two treatments and potential miRNA regulators, and we employed publicly available regulatory databases in order to gain a deeper understanding of regulatory mechanisms in driving the relapse process associated with the respective drug treatment. The cooperative functional role of the co-regulated genes during the relapse process was evaluated in terms of statistical significance and biological relevance. We also characterized the exclusive gene signatures regulated by the corresponding drug and the associated functional terms and pathways enriched in each cell line.

2. Materials and Methods

2.1. Cell Lines and Culture Conditions

Both pro-B-ALL cell lines were purchased from “Deutsche Sammlung von Mikroorganismen und Zellkulturen GmbH” (Braunschweig, Germany) and cultured according to the manufacturer’s protocol. RS4;11 was grown in Alpha-MEM Medium (Biochrom GmbH, Berlin, Germany) and SEM in Iscove’s MEM Medium (Biochrom GmbH, Berlin, Germany). Both media were supplemented with 1% penicillin/streptomycin (Biochrom GmbH, Berlin, Germany) and 10% heat-inactivated fetal bovine serum (Biochrom GmbH, Berlin, Germany). Cells were cultivated in a humidified atmosphere with 5% CO₂ at 37 °C and placed in T175 tissue culture flasks (Greiner Bio-One GmbH, Frickenhausen, Germany) in downright position.

2.2. Cytostatic Agents

Cytarabine (AraC) (100 mg/mL) was purchased from cell pharm GmbH (Bad Vilbel, Germany) and Dexamethasone (Dexa) (8 mg inject Jenapharm®) from mibe GmbH (Brehna, Germany). The cytostatics were diluted in phosphate-buffered saline (PBS) for the inhibitory experiments. Control cells were incubated with their respective medium containing the same concentration of PBS as the cells treated with the different drugs.

2.3. Drug Application Experiments

The cell lines were treated with drug concentrations similar to doses used in clinical settings. These concentrations allow for a threshold of above 30% living cells after 72 h of incubation or, alternatively, with a maximum of 10 µM. RS4;11 was incubated with either 10 µM AraC or 0.01 µM Dexa. The cell line SEM was incubated with either 0.1 µM AraC or 10 µM Dexa. For all experiments, a density of 3.33×10^5 cells/mL was used.

After 72 h incubation, cell biological analyses were performed to observe the effect on proliferation (trypan blue staining), proliferation and metabolism (WST-1 assay). Cell pellets were collected for further RNA-isolation and transcriptome sequencing. At this time point, another aliquot of the cells received new media and were incubated for another 72 h before the same readout was performed (readout 144 h).

2.4. Biological Assays (Cell Count, Proliferation and Metabolic Activities)

For the cell count analysis, RS4;11 and SEM cells were seeded at a density of 0.5×10^6 cells per 1.5 mL in 24-well plates (Greiner Bio One GmbH, Frickenhausen, Germany) at the initial time point zero (for readout at 72 h) and, after 72 h (for readout at 144 h), cells were harvested and washed in PBS (10 min, 180 × g, 4 °C), and the cell counts were determined using trypan blue staining (Sigma-Aldrich Chemie GmbH, Steinheim, Germany). An overview of the experimental setup is presented in Figure 1.

For the WST-1 proliferation assay, both cell lines were seeded in biological triplicates at a density of 5×10^4 cells per 150 µL per well in 96-well plates at the initial time point zero (readout 72 h) and after another 72 h (readout 144 h). The metabolic activity was analyzed via tetrazolium compound WST-1 (TaKaRa Bio Inc., Kusatsu, Japan), an indicator assay for the cells’ metabolic activity in comparison to the cell count. After 72 h and 144 h, the cells were incubated with 15 µL WST-1 for up to 3 h. The principle of this assay was based on the mitochondrial dehydrogenases of vital cells, which reduce the soluble WST-1 in the dark red formazan. The amount of formazan dye directly correlates to the activity and number of active metabolic cells and can be measured by photometer (absorbance: 450 nm; reference: 750 nm). As background control, we used the absorbance of pure culture medium with added WST-1. The comparison of the data of the WST-1 assay and the cell count gives hints about the metabolic activity of the cells.

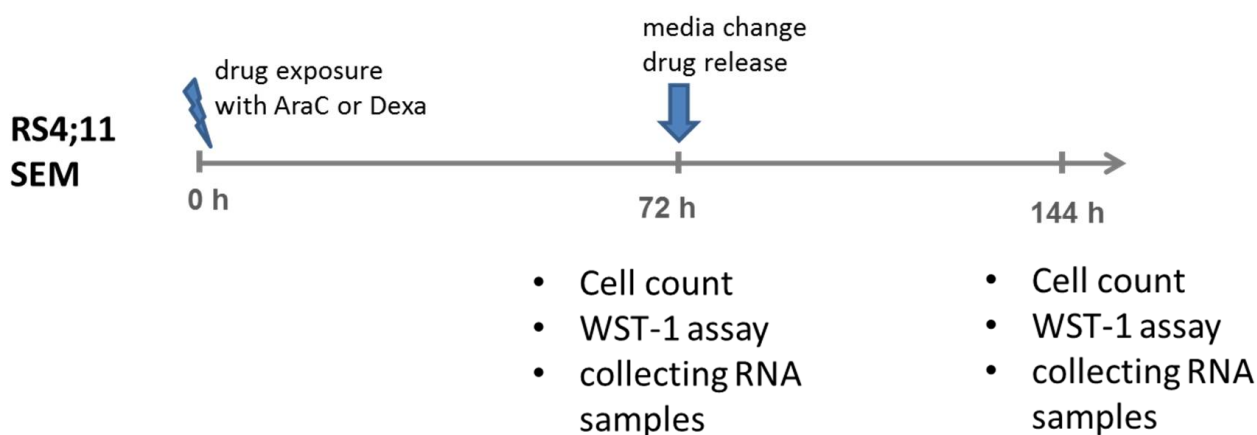


Figure 1. Schematic diagram for the experimental setup to study relapse mechanisms and identify biomarkers for relapse in pro-B-ALL. Two settings were chosen: (1) drug exposure for 72 h, followed by (2) no drug exposure (“drug release”) for an additional 72 h, noted here as 144 h (+/–). In the experimental readout, trypan-blue staining (cell count), WST-1 assay (cell count and metabolism analysis) and sample collection for following RNA-Seq of RS4;11 and SEM were performed.

2.5. RNA-Isolation and Sequencing

Control cells were cultivated in T75- tissue culture flasks and Dexa or AraC incubated cells of both cell lines were cultivated in T175-tissue culture flasks in downright position. Cells were harvested and washed (10 min, $180 \times g$, $4^\circ C$) in PBS three times. Total RNA was extracted using the miRNeasy Mini Kit (Qiagen, Hilden, Germany), as described in the Quick Start Protocol. Then, 500 μL Buffer RWT and 350 μL Buffer RPE were added twice after performing the DNase (Qiagen, Hilden, Germany) digest. The RNA quantity was assessed using the NanoDrop Spectrophotometer ND 1000 (Peqlab Biotechnologie GmbH, Erlangen, Germany, Version 3.7.1). For each condition/experiment, three biological replicates were prepared and a total of 1 μg total RNA, with RNA integrity numbers > 8 with poly-A enrichment, was used for preparing the sequencing libraries using the NEBNext Ultra RNA preparation Kit (New England Biolabs, Ipswich, MA, USA) according to the manufacturer’s protocols. The sequencing was conducted on an Illumina NextSeq500 (Illumina, San Diego, CA, USA) as single reads with 75 bp length.

2.6. Data Processing

FastQC v.0.11.5 [32] was used to evaluate the quality of the raw sequencing reads and adjust the correct adapter trimming. Trimmomatic v. 0.36 [33], with the following parameters: ILLUMINACLIP:./adapters/list.fa:2:30:10:6 LEADING:3 TRAILING:3 SLIDINGWINDOW:4:15 MINLEN:36, was applied for trimming the adapters and primers sequences. After the adapter trimming, sequence quality was checked with FastQC [32], and reads with an average Phred quality score of ≥ 30 were considered high quality. Next, all high-quality reads were mapped to the human reference genome GRCh38.78 (Ensembl) using TopHat v.2.1.1 [34]. With the combination of SAMtools v.1.3 [35] and HTSeq-count v.0.6.1p1 [36], the read counts of the mapped reads were counted per ENSEMBL-ID of the GRCh38.78. ENSEMBL-IDs were then mapped using the Bioconductor package org.Hs.eg.db v.3.5.0 [37] to the corresponding gene symbol. Differential expression gene (DEG) analysis was performed using the Bioconductor package DESeq2 v.1.12.4 [38] with an FDR threshold of 5% and \log_2 fold change of ± 1.5 .

2.7. Over-Representation Analysis (ORA)

An over-representation analysis was applied to the differentially expressed genes (DEGs) to filter out genes related to functional terms of stress release/response and metabolism (Supplement Table S1) and to highlight the enriched GO terms and pathways in each drug response. ORA was performed using DAVID as previously described by

Hamed et al., 2018 [39]. Statistical significance of the enriched terms and pathways was evaluated via Fisher's exact test followed by the Benjamini–Hochberg adjustment [40] for controlling the false discovery rate (FDR), with a cutoff value of 0.05.

2.8. miRNA Enrichment Analysis and Related ORA

The miRNAs included in the GRNs (see Section 2.9) were predicted by identifying the set of miRNAs whose target genes are statistically enriched within the DEG lists (see Section 2.6). The miRNA target-genes associations were retrieved from the regulatory databases of TFmiR [41]. The hypergeometric test followed by Benjamini–Hochberg adjustment (FDR = 5%) was used to evaluate the significance of the miRNA enrichment. The over-representation analysis for each miRNA set was performed using TAM v2.0 [42,43] to identify the functional terms and diseases enriched in each miRNA set.

2.9. Gene Regulatory Network (GRN) Construction

The TFmiR web service [41] was used to construct the GRN for each drug treatment based on the DEG set and the corresponding enriched miRNA set. We considered only the regulatory interactions that are supported by experimental evidence. We contextualized the resulting networks to leukemia by considering only regulatory interactions whose source nodes or target nodes are known to be associated with leukemia, generating a leukemia-specific network for each drug treatment. Key network drivers (central hub miRNAs/genes) were identified using the union set of nodes considering each of four network centrality measures (degree, betweenness, closeness and eigenvector) [41,44]. More specifically, for each centrality measure, we selected the top 10% genes/miRNAs of highest centrality. The GRN networks were visualized using Cytoscape v3.3.0 [45].

2.10. Semantic Validation of the GRNs Nodes

The GoSemSim R package [46] was used to compute the functional similarity scores within the GRN nodes based on their GO annotation. Nominal *p*-values for evaluating the statistical significance of the functional homogeneity of the GRN genes were calculated based on 100 random gene sets. The Kolmogorov–Smirnov test was adopted to check whether the similarity scores of GRN gene pairs were statistically higher than the scores of randomly selected pairs. The FDR was controlled using the Benjamini–Hochberg procedure [40] with a cutoff value of 0.05.

3. Results

3.1. Experimental Design and Cell Line Characteristic Biological Effects of the Used Agents

To reflect patient-relevant settings, we exposed the cell lines RS4;11 and SEM to the drugs AraC and Dexa for 72 h, followed by 72 h without chemotherapeutic pressure (drug release, noted here as 144 h+/-); see Figure 1. This setting could help to identify potential driver genes, which are responsible for relapse in response to AraC or Dexa.

In order to quantify the biological effects of the two drug applications on proliferation rate and metabolism, we set (1) the initially seeded cells as 100% in Figure 2a,d and (2) the control cells as 100% (readout 72 h and 144 h) in Figure 2b,c,e,f. In general, incubation with AraC and Dexa causes, in both cell lines, a reduced proliferation rate compared to the control cells after 72 h. The exposure of AraC in RS4;11 approximately halved the proliferation rate compared to the control. In contrast, the exposure of Dexa reduced the proliferation to 15% in comparison to the control. A low increase in metabolic activity was detected by both AraC and Dexa exposures. After 144 h in total, the AraC release (AraC +/- 144 h) resulted in nearly the same proliferation rate as the control cells, but Dexa resulted in an almost halved proliferation rate. The measurement of the metabolic activity showed, in both settings, comparable results to the proliferation rate (Figure 2c).

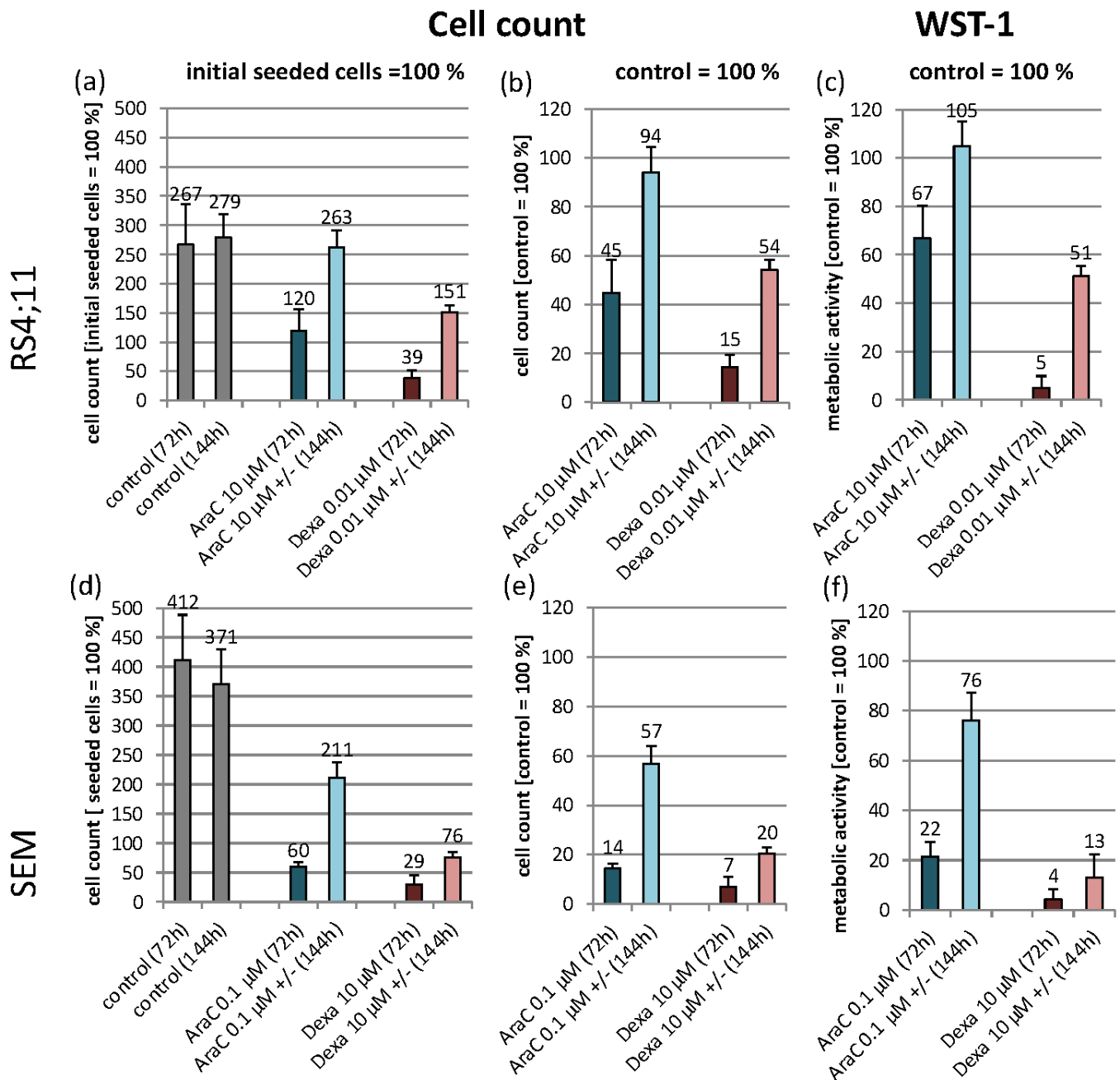


Figure 2. Cell count and metabolic activity in RS4;11 (a–c) and SEM (d–f) in response to AraC and Dexa for 72 h. After 72 h, drugs were released and cells cultivated for another 72 h (144 h+/-). Cell count (a,b,d,e) and WST-1 proliferation assay (c,f) were performed after 72 h and 144 h. The control cells and drug exposure times were compared with the Students' *t*-test at significance levels of * $p \leq 0.05$, ** $p \leq 0.01$, *** $p \leq 0.001$, [$n \geq 3$].

An AraC exposition in SEM leads to an approximately 15% proliferation rate, and Dexa to a < 10% proliferation rate compared to control cells. Comparable results were observed by measurements of the metabolic activity. The drug release resulted, after a total of 144 h, in the case of AraC, in approximately half of the proliferation rate of the control cells, but the Dexa release resulted in a quarter of the proliferation rate. Furthermore, the metabolic activity in AraC-exposed cells resulted in an increase compared to the results of the cell count (Figure 2f).

3.2. Whole-Genome Transcriptomic Differences between AraC and Dexa

To better elucidate the results of the biological assays on the molecular level, we performed a high coverage whole transcriptomic analysis of the RS4;11 and SEM cells following Dexa and AraC treatments. The PCA of the expression profiles for each drug treatment showed a clear separation between the drug responses of each cell line (Figure 3A). Interestingly, within each cell line, the samples after the 72 h drug application, as well as the corresponding samples after 72 h of drug release (144 h+/-), were clustered in different groups for each drug, indicating differences in the relapse-associated molecular response. The comparative RNA-Seq analysis of 72 h and 144 h+/- revealed genes that are dysregulated due to the stress release and metabolism, as well as potential genes involved in relapse in response to AraC and Dexa. We filtered out genes related to stress release and metabolism (see Methods) to focus our downstream analysis on relapse-associated genes. Considering the drug resistance and sensitivity of the two cell lines, marked differences in the genes potentially involved in relapse are shown in Figure 3B and File S1-Supplementary Table S2. The differential analysis revealed 2183 differentially expressed genes (DEG) in RS4;11 in response to Dexa treatment, confirming the sensitivity of the RS4;11 cell line to Dexa. Furthermore, both drugs share, considering both cell lines, 23 potential target genes, although a high amount of exclusively deregulated genes was found for each drug release in the corresponding cell line.

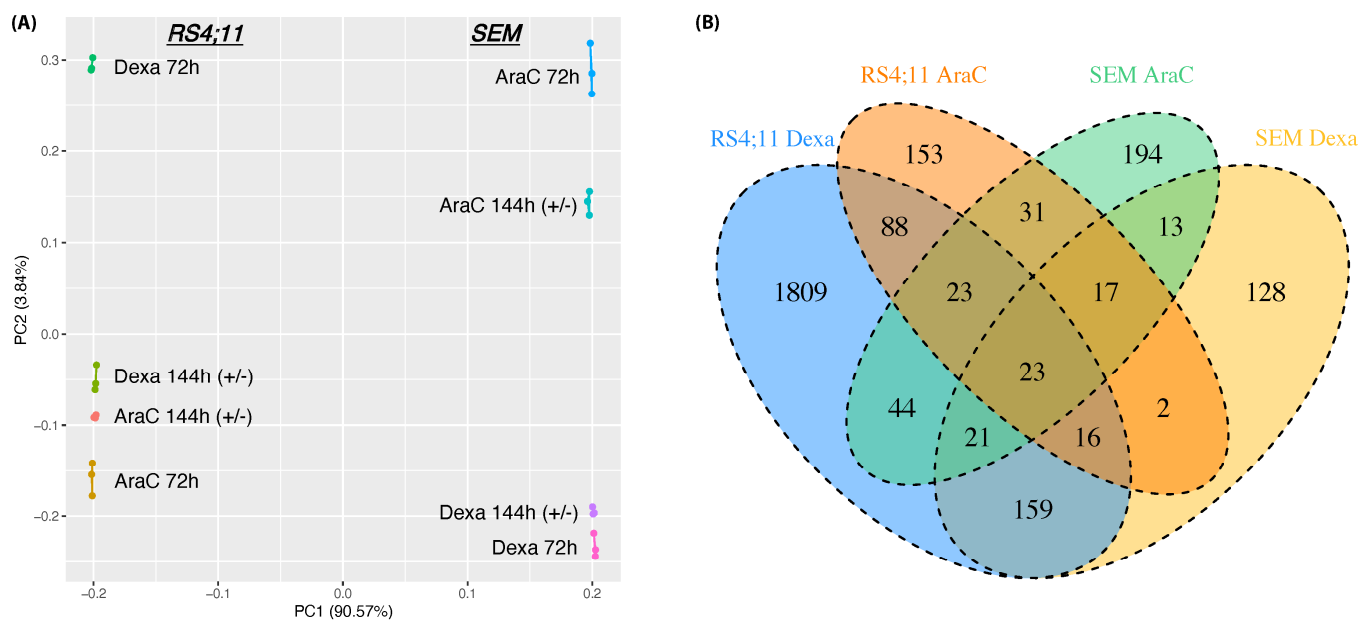


Figure 3. Dissimilarity of the transcriptional response of Dexa and AraC when applied to SEM and RS4;11. **(A)** PCA of whole transcriptome profiles of AraC and Dexa applications in the cell lines. **(B)** Venn diagram showing the differentially expressed genes (DEGs) of each drug treatment in each cell line. The experiments were carried out in biological triplicates.

3.3. Functional Relapse Characteristics in Response to Each Drug Treatment

Subsequently, an over-representation analysis was performed to investigate the GO terms (biological processes (BPs) and molecular functions (MFs)) associated with relapse due to AraC and Dexa in RS4;11 and SEM (Figure 4). The ORA revealed 66 enriched BPs and 45 enriched MFs in both cell lines. More specifically, in RS4;11, the drug release of Dexa is suggested to involve (transmembrane) protein transport and the mitochondria, whereas the drug release of AraC may influence the cell cycle, translation, chromosome segregation, protein targeting and microtubule organization. The drug release of Dexa in SEM may engage morphogenesis and the microtubule bundle, whereas AraC may encompass antigen presentation and chromosome/chromatin/centromere/histone organization. With respect

to molecular functions, the Dexa release suggests a modulation in channel and transporter activities whereas the AraC release may involve phosphate/GTPase activity, ribosome and RNA binding in the RS4;11 cell line. In the SEM cell line, the Dexa release revealed that metal ion/cation/ion binding and transmembrane transporter and symporter may be involved in the relapse process, whereas the AraC release may involve hydrolase/galactosyl activity and the microtubule.

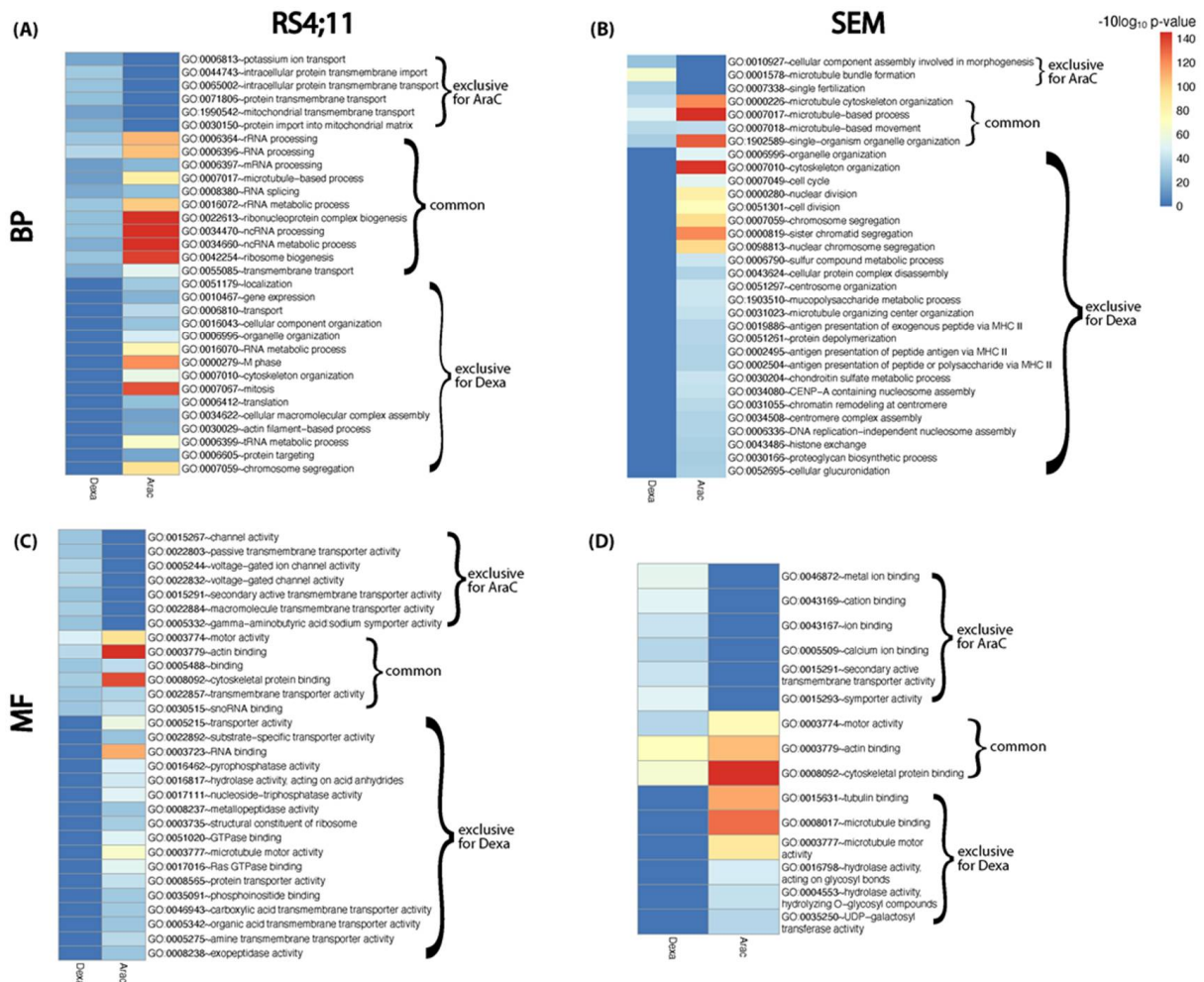


Figure 4. Over-represented biological processes and molecular functions for the cell lines RS4;11 (A) and for SEM (B) shown separately for the exclusive patterns for the drug releases of AraC and Dexa, as well as the common ones. The molecular functions for RS4;11 (C) and SEM (D) in response to the drug release of AraC and Dexa differentiating between common and exclusive over-representation.

3.4. miRNA Enrichment Analysis

We further identified enriched miRNAs in each DEG set from the aforementioned analyses by determining the list of miRNAs whose target genes are significantly enriched within the DEG sets. The biological role of these miRNAs was postulated by linking them to functional and disease annotations via an ORA (File S1 Supplementary Tables S3–S6). Interestingly, the identified miRNAs in both cell lines and drug treatments were significantly associated with primary effusion lymphoma ($p < 1.39 \times 10^{-9}$), acute myeloid leukemia ($p < 0.0113$) and chronic myeloid leukemia ($p < 3.29 \times 10^{-4}$). The biological functions of the enriched miRNAs of the AraC-related response were hematopoiesis ($p < 5.95 \times 10^{-3}$), immune response ($p < 0.0108$), inflammation ($p < 0.027$) and cell proliferation ($p < 5.45 \times 10^{-3}$).

For the Dexa-related response, apoptosis ($p < 0.0145$), inflammation ($p < 1.27 \times 10^{-3}$) and the tumor suppressor miRNAs ($p < 6.60 \times 10^{-3}$) were significantly enriched.

3.5. Construction of Relapse-Mediated Gene Regulatory Networks (GRN)

Next, we constructed GRNs that combine transcriptional and post-transcriptional regulatory interactions between the dysregulated genes and the corresponding enriched miRNAs and contextualized them to leukemia (see Methods). Moreover, we ranked the genes/miRNAs according to their node centrality in order to consider their putative mechanistic impact and to characterize the central hub nodes (the “hotspots”) that drive the dynamic regulation of the relapse process after the release of drug pressure, and that therefore potentially act as master regulators.

The exclusive regulatory modulation in response to AraC treatment revealed, in RS4;11, a GRN based on two miRNAs (hsa-mir-370, hsa-let7e) and three hotspot driver genes (RIMS3, DHX35, HSPA12A) (Figure 5A), whereas, in SEM, the GRN consists of three miRNAs (mir-30a, mir-370, mir-34b) and seven hotspot driver genes (LIMCH1, NAV1, CCDC107, SHROOM4, MARCKS, BEX2, PLEKHA6) (Figure 5B). For the GC-sensitive RS4;11 cell line, we constructed a regulatory network comprising 95 hotspot genes and 28 hotspot miRNAs (Figure 5C). In contrast, for the SEM cells, four hotspot miRNAs (mir-31, mir-410, let-7b, let-7c) and six hotspot driver genes (TTC33, DYNC111, QSERV, LOXL4, AGPS, MYRIP) were identified (Figure 5D).

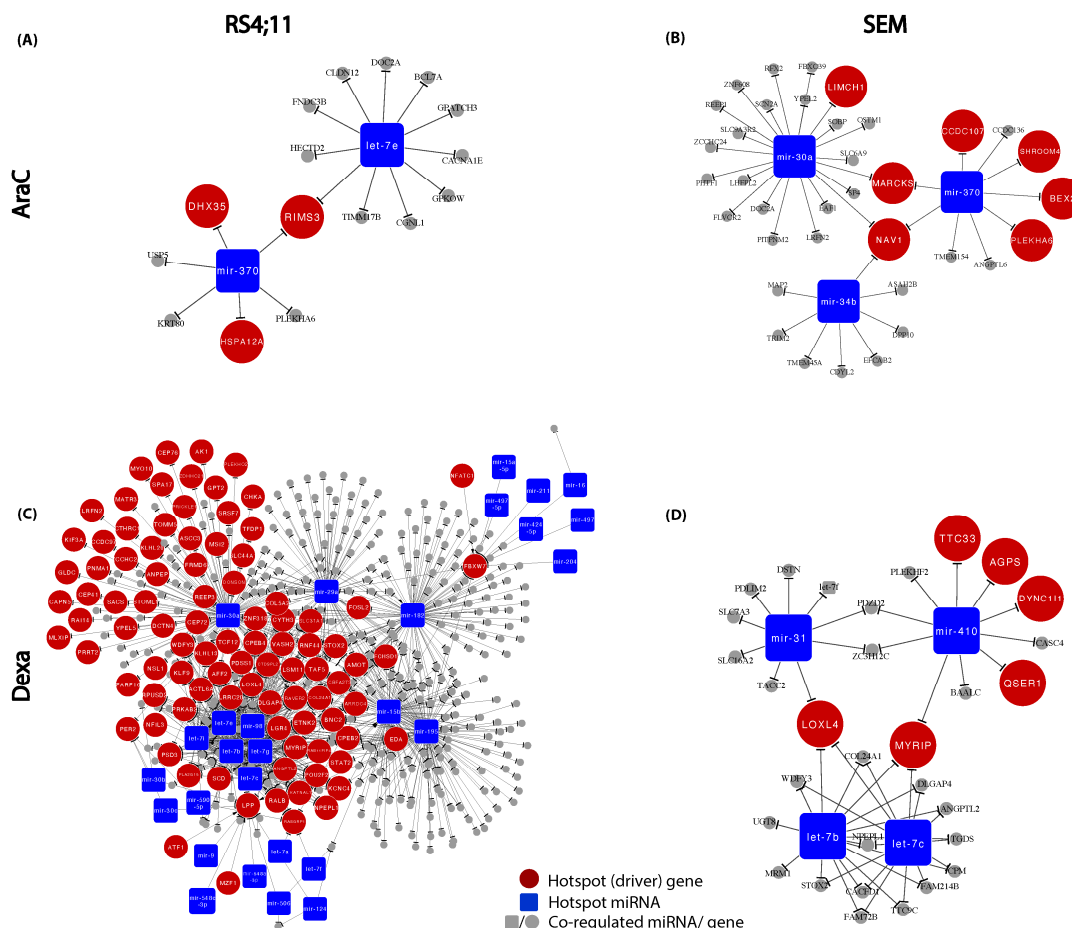


Figure 5. GRNs in response to AraC and Dexa in RS4;11 and SEM. Large red nodes represent the hotspot (driver) genes, blue squares indicate hotspot miRNAs and grey nodes denote the co-regulated miRNAs/genes for (A) AraC in RS4;11, (B) AraC in SEM, (C) Dexa in RS4;11 and (D) Dexa in SEM.

3.6. Functional Similarity and Integrity between the Relapse-Mediated GRN Genes

We further assessed the biological relevance and the cooperative functional roles of the genes and miRNAs that may be involved in the relapse-mediated GRNs. For each GRN, we computed the functional similarity scores between all gene pairs, including the miRNA target genes. By comparing the resulting score distribution with the similarity score distribution of randomly selected gene pairs, we found that the GRN genes and the miRNA targets have significantly more functional similarity than the randomly selected pairs (p -values $< 3.9 \times 10^{-3}$, Kolmogorov–Smirnov test), Figure 6. This implies the functional homogeneity and integrity within the GRN genes and miRNAs, representing the molecular interactions and dysregulation mechanisms that may underlie the relapse process associated with each treatment.

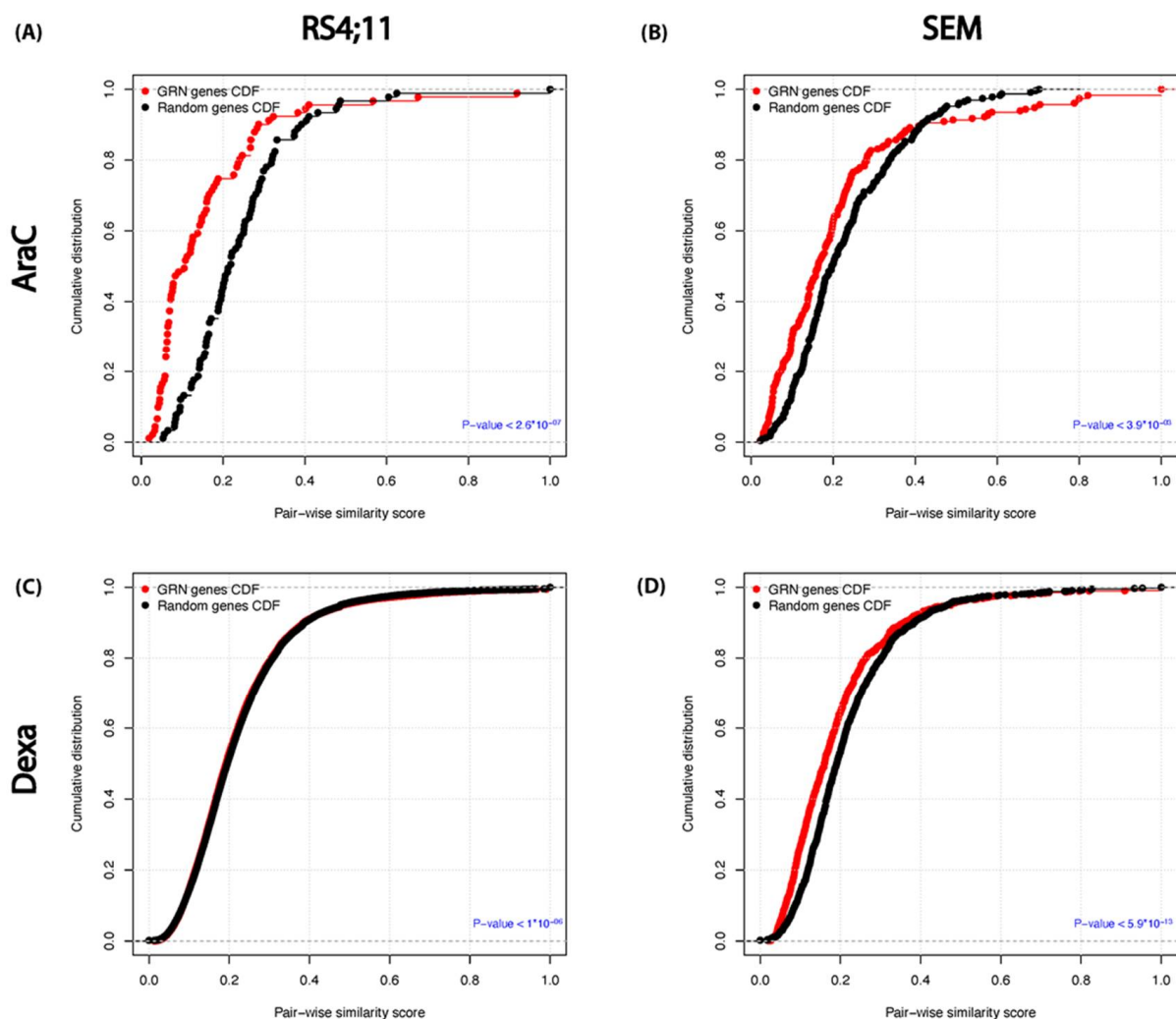


Figure 6. The functional homogeneity within each drug–GRN in the two examined cell lines. For each GRN, the cumulative distribution of GO functional semantic scores of gene pairs of the GRN (red) versus randomly selected genes (black) are depicted for (A) AraC in RS4;11, (B) AraC in SEM, (C) Dexa in RS4;11 and (D) Dexa in SEM. The corresponding p -values were calculated using the Kolmogorov–Smirnov test. The GRNs were constructed with the TFmiR web service (41) for each drug treatment based on the DEG set and the corresponding enriched miRNA set, and visualized using Cytoscape V3.3.0 [45].

4. Discussion

In this study, we used the cell lines RS4;11 and SEM isolated from relapsed patients to mimic an unfavorable clinical phenotype (KMT2A (also known as MLL) rearrangement) in adult and childhood pro-B-ALL and to study the effect of the drug release (144 h (+/−)) of the nucleoside analog AraC and the glucocorticoid Dexa. We examined the potential roles of deregulated genes and miRNAs, which may be involved in the tumor relapse for B-ALL, by identifying (1) proliferation and metabolism rates, (2) enriched biological processes (BPs) and molecular function (MF) terms based on DEGs, (3) relapse-mediating regulatory interactions (GRN) and (4) hotspot genes and miRNAs that could potentially drive the relapse mechanisms.

While proliferation increased after a drug pressure release of AraC, it was still reduced after a Dexa release. Metabolic assays revealed minor activity for the AraC treatment and a slight decrease for Dexa. Both measurements clearly showed the corresponding drug sensitivity/resistance of the cell lines. The ORA identified different BPs and MFs terms that could be involved in the B-ALL relapse mechanism after each drug release. For instance, AraC's release is mainly associated with the BP terms cell cycle, translation and antigen presentation, whereas Dexa's release is mostly associated with transmembrane-related mechanisms and microtubule bundles. Further, each drug release influences different MFs, such as ribosome and RNA binding for AraC's release and channel/transporter activities and ion binding for Dexa.

Unexpectedly, the MF term “mesenchymal stem cell proliferation” is suggested to be triggered by AraC's release in RS4;11. This specific function was reported before to be associated with the progression of AML [47,48]. In concordance with the fact that Dexa causes cell toxicity [49,50], our enrichment analysis revealed related BPs, such as toxicity and cell mortality [51]. These functions highlight the differences between childhood and adult B-ALL, mainly giving possible insights into the effect of drug release and related tumor progression in adult B-ALL besides Dexa's potential for severe side effects.

The molecular differences between the release of both agents become even more evident by constructing their putative relapse-mediated GRNs and identifying the corresponding hotspot genes and miRNAs that likely control the subsequent relapse process. The following is known about the miRNAs highlighted in Figure 5. hsa-mir-370 is linked to the response to chemotherapy [52] and chemosensitivity [53]; hsa-mir-30a is a tumor suppressor [54] found to be mainly associated with better overall survival [55–57], poor prognosis [58], early recurrence [59] and response to chemotherapy [60]; hsa-mir-34b plays an essential role regarding tumor progression [61,62] and recurrence [63]; miRNAs hsa-mir-124, hsa-mir-9 and hsa-mir-29a are mainly associated with shorter survival [64], poor prognosis [65,66], GC resistance [67] and a higher amount of blasts in the bone marrow [68]. Furthermore, the hsa-mir-15/16 family is responsible for an insufficient response to chemotherapy and shorter survival [69], a poor prognosis [70], and it is correlated with BCL2 expression, which leads to apoptosis resistance [64]; hsa-mir-410 was previously shown to have a key role in proliferation, colony formation and the apoptosis of ALL cancerous cells [71], and the hsa-let-7 family is known as tumor suppressor miRNAs influencing chemosensitivity [72,73].

Interestingly, some of the genes, such as angiomin (AMOT), adenylate kinase 1 (AK1), Musashi RNA binding protein (MSI), signal transducer and activator of transcription (STAT2) and POU class 2 homeobox 2 (POU2F2), were reported before as cancer survival markers [74–80], whereas other genes, such as F-box and WD repeat domain containing 7 (FBXW7) and choline kinase alpha (CHKA), were found to be regulated by GC treatment [23,71,81]. Myristoylated alanine rich protein kinase C substrate (MARCKS) is of high relevance due to being associated with drug resistance [82,83], as well as being a target gene to improve clinical outcome [84,85]. Some genes are known risk markers, such as myosin VIIA And rab interacting protein (MYRIP) for infant ALL [86], or alkylglycerone phosphate synthase (AGPS) for shorter survival [87].

Study limitations. The main limitation of any study based on in vitro data is the missing confirmation of the insights in an in vivo (animal, xenograft or patient) setting. At this moment, some confidence can be based on the plausibility of many of our findings, given the literature-based discussion above. Within the in vitro setting, it would of course be useful to test far more cell lines, drugs and timings of drug application; however, resources are limited. Regarding the bioinformatics analyses, an array of straightforward canonical analyses was performed, and insightful network-biology approaches were executed. However, the choice of further potential analyses is vast. Then again, the basic insights of our analyses matched a lot of knowledge already reported in the literature, so alternative analyses are expected to yield results that, to a sufficient degree, are expected to match the ones reported.

5. Conclusions

In conclusion, we revealed molecular differences in drug release and possible subsequent relapse-mediated mechanisms in response to two cytostatic agents (AraC and Dexa) in two B-ALL cell line models, highlighting candidate genetic drivers of the ALL progression with respect to the age of onset (childhood and adults). The constructed relapse-mediated GRNs for each agent were assessed for their functional homogeneity and literature evidence. This regulatory analysis helped us to spot genes and miRNAs that are exclusively deregulated by the two agents in the selected settings. Further wet lab experiments are warranted to test the usefulness of these genes and miRNAs as therapeutic targets and/or prognosis indicators in B-ALL. They may ultimately be used to develop a superior application protocol to best treat the patient.

Supplementary Materials: The following supporting information can be downloaded at: <https://www.mdpi.com/article/10.3390/genes13071240/s1>, File S1, Supplementary Table S1: Gene Ontology terms related to stress release and metabolism as reported in DAVID; Supplementary Table S2: Number of DEGs before and after filtration for drug/stress release and metabolism; Supplementary Table S3: miRNA enrichment for the AraC drug release in RS4;11; Supplementary Table S4: miRNA enrichment for the Dexa drug release in RS4;11; Supplementary Table S5: miRNA enrichment for the AraC drug release in SEM; Supplementary Table S6: miRNA enrichment for the Dexa drug release in SEM. File S2, the processed RNASeq data used in this study.

Author Contributions: Y.S.G.: conceptualization, methodology, software, formal analysis, investigation, data curation, writing—original draft, visualization; L.-M.S.: conceptualization, methodology, formal analysis, investigation, writing—original draft; C.R.: resources; J.B.: resources, writing—review and editing; E.S.: resources, writing—review and editing; G.F.: resources, writing—review and editing, project administration, funding acquisition; C.J.: resources, writing—review and editing, project administration, funding acquisition; H.M.E.: conceptualization, methodology, investigation, writing—review and editing, resources, supervision, project administration, funding acquisition; M.H.: conceptualization, methodology, investigation, writing—original draft, writing—review and editing, resources, supervision, project administration. All authors have read and agreed to the published version of the manuscript.

Funding: BMBF: VIP—Validierung des Innovationspotentials wissenschaftlicher Forschung (03V0396). LMS: Supported by “Professorinnenprogramm Universität Rostock”. Support for computing equipment was provided by the European Union (EFRE, “European Fund for Regional Development”, Grant number GHS-15-0019, 2016-2021).

Institutional Review Board Statement: Not applicable.

Informed Consent Statement: Not applicable.

Data Availability Statement: The RNA-Seq data are provided in Supplementary File S2.

Acknowledgments: We thank Anett Sekora, Gudrun Knübel, Sina Sender and Anna-Marie Merken-schlager for their technical assistance.

Conflicts of Interest: The authors declare that the research was conducted in the absence of any commercial or financial relationships that could be construed as a potential conflict of interest.

References

1. Gökbuget, N.; Hoelzer, D. Treatment of Adult Acute Lymphoblastic Leukemia. *Semin. Hematol.* **2009**, *46*, 64–75. [[CrossRef](#)] [[PubMed](#)]
2. Hoelzer, D.; Gökbuget, N. Chemoimmunotherapy in acute lymphoblastic leukemia. *Blood Rev.* **2012**, *26*, 25–32. [[CrossRef](#)] [[PubMed](#)]
3. Gökbuget, N. Treatment of older patients with acute lymphoblastic leukemia. *Hematology* **2016**, *2016*, 573–579. [[CrossRef](#)] [[PubMed](#)]
4. Jacobson, S.; Tedder, M.; Eggert, J. Adult Acute Lymphoblastic Leukemia: A Genetic Overview and Application to Clinical Practice. *Clin. J. Oncol. Nurs.* **2016**, *20*, E147–E154. [[CrossRef](#)] [[PubMed](#)]
5. Müschen, M. Rationale for targeting the pre-B-cell receptor signaling pathway in acute lymphoblastic leukemia. *Blood* **2015**, *125*, 3688–3693. [[CrossRef](#)]
6. Cruz-Rodriguez, N.; Combata, A.L.; Enciso, L.J.; Quijano, S.M.; Pinzon, P.L.; Lozano, O.C.; Castillo, J.S.; Li, L.; Bareño, J.; Cardozo, C.; et al. High expression of ID family and IGJ genes signature as predictor of low induction treatment response and worst survival in adult Hispanic patients with B-acute lymphoblastic leukemia. *J. Exp. Clin. Cancer Res.* **2016**, *35*, 64. [[CrossRef](#)]
7. Inaba, H.; Greaves, M.; Mullighan, C.G. Acute lymphoblastic leukaemia. *Lancet* **2013**, *381*, 1943–1955. [[CrossRef](#)]
8. Fruman, D.A.; Rommel, C. PI3K and cancer: Lessons, challenges and opportunities. *Nat. Rev. Drug Discov.* **2014**, *13*, 140–156. [[CrossRef](#)]
9. Winters, A.C.; Bernt, K.M. MLL-Rearranged Leukemias—An Update on Science and Clinical Approaches. *Front. Pediatrics* **2017**, *5*, 4. [[CrossRef](#)]
10. Spijkers-Hagelstein, J.A.P.; Pinhanços, S.S.; Schneider, P.; Pieters, R.; Stam, R.W. Chemical genomic screening identifies LY294002 as a modulator of glucocorticoid resistance in MLL-rearranged infant ALL. *Leukemia* **2013**, *28*, 761–769. [[CrossRef](#)]
11. Hoelzer, D.; Bassan, R.; Dombret, H.; Fielding, A.; Ribera, J.-M.; Buske, C.; ESMO Guidelines Committee. Acute lymphoblastic leukaemia in adult patients: ESMO Clinical Practice Guidelines for diagnosis, treatment and follow-up. *Ann. Oncol.* **2016**, *27*, v69–v82. [[CrossRef](#)] [[PubMed](#)]
12. Torra, O.S.; Othus, M.; Williamson, D.W.; Wood, B.; Kirsch, I.; Robins, H.; Beppu, L.; O'Donnell, M.R.; Forman, S.J.; Appelbaum, F.R.; et al. Next-Generation Sequencing in Adult B Cell Acute Lymphoblastic Leukemia Patients. *Biol. Blood Marrow Transplant.* **2017**, *23*, 691–696. [[CrossRef](#)] [[PubMed](#)]
13. Mohseni, M.; Uludag, H.; Brandwein, J.M. Advances in biology of acute lymphoblastic leukemia (ALL) and therapeutic implications. *Am. J. Blood Res.* **2018**, *8*, 29–56. [[PubMed](#)]
14. Terwilliger, T.; Abdul-Hay, M. Acute lymphoblastic leukemia: A comprehensive review and 2017 update. *Blood Cancer J.* **2017**, *7*, e577. [[CrossRef](#)] [[PubMed](#)]
15. Sklarz, L.-M.; Gladbach, Y.S.; Ernst, M.; Hamed, M.; Roof, C.; Sender, S.; Beck, J.; Schütz, E.; Fischer, S.; Struckmann, S.; et al. Combination of the PI3K inhibitor idelalisib with the conventional cytostatics cytarabine and dexamethasone leads to pathway modulations inducing anti-proliferative effects in B lymphoblastic leukaemia cell lines. *Cancer Cell Int.* **2020**, *20*, 1–14. [[CrossRef](#)]
16. Pui, C.-H.; Yang, J.J.; Hunger, S.P.; Pieters, R.; Schrappe, M.; Biondi, A.; Vora, A.; Baruchel, A.; Silverman, L.B.; Schmiegelow, K.; et al. Childhood Acute Lymphoblastic Leukemia: Progress through Collaboration. *J. Clin. Oncol.* **2015**, *33*, 2938–2948. [[CrossRef](#)]
17. Mitchell, C.D.; Richards, S.M.; Kinsey, S.E.; Lilleyman, J.; Vora, A.; Eden, T.O.B.; The Medical Research Council Childhood Leukaemia Working Party. Benefit of dexamethasone compared with prednisolone for childhood acute lymphoblastic leukaemia: Results of the UK Medical Research Council ALL97 randomized trial. *Br. J. Haematol.* **2005**, *129*, 734–745. [[CrossRef](#)]
18. Vrooman, L.M.; Stevenson, K.E.; Supko, J.G.; O'Brien, J.; Dahlberg, S.E.; Asselin, B.L.; Athale, U.H.; Clavell, L.A.; Kelly, K.M.; Kutok, J.L.; et al. Postinduction Dexamethasone and Individualized Dosing of *Escherichia Coli* L-Asparaginase Each Improve Outcome of Children and Adolescents With Newly Diagnosed Acute Lymphoblastic Leukemia: Results From a Randomized Study—Dana-Farber Cancer Institute ALL Consortium Protocol 00-01. *J. Clin. Oncol.* **2013**, *31*, 1202–1210. [[CrossRef](#)]
19. Inaba, H.; Pui, C.-H. Glucocorticoid use in acute lymphoblastic leukaemia. *Lancet Oncol.* **2010**, *11*, 1096–1106. [[CrossRef](#)]
20. Berger, D.P.; Engelhardt, R.; Mertelsmann, R. Das Rote Buch-Hämatologische und Internistische Onkologie. In *Das Rote Buch-Hämatologische und Internistische Onkologie*, 6th ed.; Ecomed-Storck GmbH: Landsberg am Lech, Germany, 2017.
21. Stanulla, M.; Schrappe, M. Treatment of Childhood Acute Lymphoblastic Leukemia. *Semin. Hematol.* **2009**, *46*, 52–63. [[CrossRef](#)]
22. Gibson, T.M.; Ehrhardt, M.J.; Ness, K.K. Obesity and Metabolic Syndrome Among Adult Survivors of Childhood Leukemia. *Curr. Treat. Options Oncol.* **2016**, *17*, 1–13. [[CrossRef](#)] [[PubMed](#)]
23. Dyczynski, M.; Vesterlund, M.; Björklund, A.-C.; Zachariadis, V.; Janssen, J.; Gallart-Ayala, H.; Daskalaki, E.; Wheelock, C.E.; Lehtiö, J.; Grandér, D.; et al. Metabolic reprogramming of acute lymphoblastic leukemia cells in response to glucocorticoid treatment. *Cell Death Dis.* **2018**, *9*, 1–13. [[CrossRef](#)] [[PubMed](#)]
24. Brissot, E.; Ito, S.; Lu, K.; Cantilena, C.; Smith, B.D.; Prince, G.; Sadrzadeh, H.; Fathi, A.T.; Strickland, S.A.; Hensel, N.F.; et al. T Cell Exhaustion and Downregulation of Cytotoxic NK Cells—An Immune Escape Mechanism in Adult Acute Lymphoblastic Leukemia. *Blood* **2014**, *124*, 3781. [[CrossRef](#)]
25. Ragusa, D.; Makarov, E.M.; Britten, O.; Moralli, D.; Green, C.M.; Tosi, S. The RS4;11 cell line as a model for leukaemia with t(4;11)(q21;q23): Revised characterisation of cytogenetic features. *Cancer Rep.* **2019**, *2*, e1207. [[CrossRef](#)]

26. Bhatla, T.; Wang, J.; Morrison, D.J.; Raetz, E.A.; Burke, M.J.; Brown, P.; Carroll, W.L. Epigenetic reprogramming reverses the relapse-specific gene expression signature and restores chemosensitivity in childhood B-lymphoblastic leukemia. *Blood* **2012**, *119*, 5201–5210. [CrossRef]
27. Stumpel, D.J.; Schneider, P.; Pieters, R.; Stam, R.W. The potential of clofarabine in MLL-rearranged infant acute lymphoblastic leukaemia. *Eur. J. Cancer* **2015**, *51*, 2008–2021. [CrossRef]
28. Wander, P.; Cheung, L.C.; Pinhanços, S.S.; Jones, L.; Kerstjens, M.; Arentsen-Peters, S.T.; Singh, S.; Chua, G.-A.; Castro, P.G.; Schneider, P.; et al. Preclinical efficacy of gemcitabine in MLL-rearranged infant acute lymphoblastic leukemia. *Leukemia* **2020**, *34*, 2898–2902. [CrossRef] [PubMed]
29. Marke, R.; Havinga, J.; Cloos, J.; Demkes, M.; Poelmans, G.; Yuniati, L.; Schenau, D.V.I.; Sonneveld, E.; Waanders, E.; Pieters, R.; et al. Tumor suppressor IKZF1 mediates glucocorticoid resistance in B-cell precursor acute lymphoblastic leukemia. *Leukemia* **2015**, *30*, 1599–1603. [CrossRef]
30. Kruth, K.A.; Fang, M.; Shelton, D.N.; Abu-Halawa, O.; Mahling, R.; Yang, H.; Weissman, J.S.; Loh, M.L.; Müschen, M.; Tasian, S.K.; et al. Suppression of B-cell development genes is key to glucocorticoid efficacy in treatment of acute lymphoblastic leukemia. *Blood* **2017**, *129*, 3000–3008. [CrossRef]
31. Hall, C.P.; Reynolds, C.P.; Kang, M.H. Modulation of Glucocorticoid Resistance in Pediatric T-cell Acute Lymphoblastic Leukemia by Increasing BIM Expression with the PI3K/mTOR Inhibitor BEZ235. *Clin. Cancer Res.* **2016**, *22*, 621–632. [CrossRef]
32. Andrews, S.; Krueger, F.; Segonds-Pichon, A.; Biggins, L.; Krueger, C.; Wingett, S. FastQC: A Quality Control Tool for High Throughput Sequence Data. 2010. Available online: <http://www.bioinformatics.babraham.ac.uk/projects/> (accessed on 1 March 2020).
33. Bolger, A.M.; Lohse, M.; Usadel, B. Trimmomatic: A flexible trimmer for Illumina sequence data. *Bioinformatics* **2014**, *30*, 2114–2120. [CrossRef] [PubMed]
34. Kim, D.; Pertea, G.; Trapnell, C.; Pimentel, H.; Kelley, R.; Salzberg, S.L. TopHat2: Accurate alignment of transcriptomes in the presence of insertions, deletions and gene fusions. *Genome Biol.* **2013**, *14*, R36. [CrossRef] [PubMed]
35. Li, H.; Handsaker, B.; Wysoker, A.; Fennell, T.; Ruan, J.; Homer, N.; Marth, G.; Abecasis, G.; Durbin, R.; 1000 Genome Project Data Processing Subgroup. The Sequence Alignment/Map format and SAMtools. *Bioinformatics* **2009**, *25*, 2078–2079. [CrossRef] [PubMed]
36. Anders, S.; Pyl, P.T.; Huber, W. HTSeq—A Python framework to work with high-throughput sequencing data. *Bioinformatics* **2015**, *31*, 166–169. [CrossRef] [PubMed]
37. Carlson, M. org.Hs.eg.db: Genome wide annotation for Human. *R Package Version* **2015**, *312*. [CrossRef]
38. Love, M.I.; Huber, W.; Anders, S. Moderated estimation of fold change and dispersion for RNA-seq data with DESeq2. *Genome Biol.* **2014**, *15*, 550. [CrossRef]
39. Hamed, M.; Trumm, J.; Spaniol, C.; Sethi, R.; Irhimeh, M.R.; Fuellen, G.; Paulsen, M.; Helms, V. Linking Hematopoietic Differentiation to Co-Expressed Sets of Pluripotency-Associated and Imprinted Genes and to Regulatory microRNA-Transcription Factor Motifs. *PLoS ONE* **2017**, *12*, e0166852. [CrossRef]
40. Benjamini, Y.; Hochberg, Y. Controlling the False Discovery Rate: A Practical and Powerful Approach to Multiple Testing. *J. R. Stat. Soc. Ser. B* **1995**, *57*, 289–300. [CrossRef]
41. Hamed, M.; Spaniol, C.; Nazarieh, M.; Helms, V. TFmiR: A web server for constructing and analyzing disease-specific transcription factor and miRNA co-regulatory networks. *Nucleic Acids Res.* **2015**, *43*, W283–W288. [CrossRef]
42. Lu, M.; Shi, B.; Wang, J.; Cao, Q.; Cui, Q. TAM: A method for enrichment and depletion analysis of a microRNA category in a list of microRNAs. *BMC Bioinform.* **2010**, *11*, 419. [CrossRef]
43. Li, J.; Han, X.; Wan, Y.; Zhang, S.; Zhao, Y.; Fan, R.; Cui, Q.; Zhou, Y. TAM 2.0: Tool for MicroRNA set analysis. *Nucleic Acids Res.* **2018**, *46*, W180–W185. [CrossRef] [PubMed]
44. Nazarieh, M.; Wiese, A.; Will, T.; Hamed, M.; Helms, V. Identification of key player genes in gene regulatory networks. *BMC Syst. Biol.* **2016**, *10*, 88. [CrossRef] [PubMed]
45. Smoot, M.E.; Ono, K.; Ruscheinski, J.; Wang, P.-L.; Ideker, T. Cytoscape 2.8: New features for data integration and network visualization. *Bioinformatics* **2010**, *27*, 431–432. [CrossRef]
46. Yu, G.; Li, F.; Qin, Y.; Bo, X.; Wu, Y.; Wang, S. GOSemSim: An R package for measuring semantic similarity among GO terms and gene products. *Bioinformatics* **2010**, *26*, 976–978. [CrossRef] [PubMed]
47. Brenner, A.K.; Nepstad, I.; Bruserud, Ø. Mesenchymal Stem Cells Support Survival and Proliferation of Primary Human Acute Myeloid Leukemia Cells through Heterogeneous Molecular Mechanisms. *Front. Immunol.* **2017**, *8*, 106. [CrossRef]
48. Lee, M.W.; Ryu, S.; Kim, D.S.; Lee, J.W.; Sung, K.W.; Koo, H.H.; Yoo, K.H. Mesenchymal stem cells in suppression or progression of hematologic malignancy: Current status and challenges. *Leukemia* **2019**, *33*, 597–611. [CrossRef]
49. Chiarini, F.; Lonetti, A.; Evangelisti, C.; Buontempo, F.; Orsini, E.; Evangelisti, C.; Cappellini, A.; Neri, L.M.; McCubrey, J.A.; Martelli, A.M. Advances in understanding the acute lymphoblastic leukemia bone marrow microenvironment: From biology to therapeutic targeting. *Biochim. Biophys. Acta* **2016**, *1863*, 449–463. [CrossRef]
50. Passaro, D.; Irigoyen, M.; Catherinet, C.; Gachet, S.; Da Costa De Jesus, C.; Lasgi, C.; Tran Quang, C.; Ghysdael, J. CXCR4 is required for leukemia-initiating cell activity in T cell acute lymphoblastic leukemia. *Cancer Cell* **2015**, *27*, 769–779. [CrossRef]

51. LaBar, B.; Suci, S.; Willemze, R.; Muus, P.; Marie, J.-P.; Fillet, G.; Berneman, Z.; Jaksic, B.; Feremans, W.; Bron, M.; et al. Dexamethasone compared to prednisolone for adults with acute lymphoblastic leukemia or lymphoblastic lymphoma: Final results of the ALL-4 randomized, phase III trial of the EORTC Leukemia Group. *Haematologica* **2010**, *95*, 1489–1495. [[CrossRef](#)]
52. Molina-Pinelo, S.; Carnero, A.; Rivera, F.; Estevez-Garcia, P.; Bozada, J.M.; Limon, M.L.; Benavent, M.; Gómez, J.; Pastor, M.D.; Chaves, M.; et al. MiR-107 and miR-99a-3p predict chemotherapy response in patients with advanced colorectal cancer. *BMC Cancer* **2014**, *14*, 656. [[CrossRef](#)]
53. Chen, X.-P.; Chen, Y.-G.; Lan, J.-Y.; Shen, Z.-J. MicroRNA-370 suppresses proliferation and promotes endometrioid ovarian cancer chemosensitivity to cisplatin by negatively regulating ENG. *Cancer Lett.* **2014**, *353*, 201–210. [[CrossRef](#)] [[PubMed](#)]
54. Ortega, M.; Bhatnagar, H.; Lin, A.P.; Wang, L.; Aster, J.C.; Sill, H.; Aguiar, R.C.T. A microRNA-mediated regulatory loop modulates NOTCH and MYC oncogenic signals in B- and T-cell malignancies. *Leukemia* **2015**, *29*, 968–976. [[CrossRef](#)] [[PubMed](#)]
55. Li, X.; Zhang, Y.; Zhang, Y.; Ding, J.; Wu, K.; Fan, D. Survival prediction of gastric cancer by a seven-microRNA signature. *Gut* **2010**, *59*, 579–585. [[CrossRef](#)] [[PubMed](#)]
56. Kawaguchi, T.; Yan, L.; Qi, Q.; Peng, X.; Gabriel, E.M.; Young, J.; Liu, S.; Takabe, K. Overexpression of suppressive microRNAs, miR-30a and miR-200c are associated with improved survival of breast cancer patients. *Sci. Rep.* **2017**, *7*, 15945. [[CrossRef](#)] [[PubMed](#)]
57. Teufel, M.; Seidel, H.; Köchert, K.; Meinhardt, G.; Finn, R.S.; Llovet, J.M.; Bruix, J. Biomarkers Associated With Response to Regorafenib in Patients With Hepatocellular Carcinoma. *Gastroenterology* **2019**, *156*, 1731–1741. [[CrossRef](#)]
58. Tang, R.; Liang, L.; Luo, D.; Feng, Z.; Huang, Q.; He, R.; Gan, T.; Yang, L.; Chen, G. Downregulation of MiR-30a is Associated with Poor Prognosis in Lung Cancer. *Med. Sci. Monit.* **2015**, *21*, 2514–2520. [[CrossRef](#)]
59. Pérez-Rivas, L.G.; Jerez, J.M.; Carmona, R.; De Luque, V.; Vicioso, L.; Claros, M.G.; Viguera, E.; Pajares, B.; Sánchez, A.; Ribelles, N.; et al. A microRNA Signature Associated with Early Recurrence in Breast Cancer. *PLoS ONE* **2014**, *9*, e91884. [[CrossRef](#)]
60. Wang, T.; Chen, G.; Ma, X.; Yang, Y.; Chen, Y.; Peng, Y.; Bai, Z.; Zhang, Z.; Pei, H.; Guo, W. miR-30a regulates cancer cell response to chemotherapy through SNAIL/IRS1/AKT pathway. *Cell Death Dis.* **2019**, *10*, 153. [[CrossRef](#)]
61. Forno, I.; Ferrero, S.; Russo, M.V.; Gazzano, G.;angiobbe, S.; Montanari, E.; Del Nero, A.; Rocco, B.M.C.; Albo, G.; Languino, L.R.; et al. Deregulation of MiR-34b/Sox2 Predicts Prostate Cancer Progression. *PLoS ONE* **2015**, *10*, e0130060. [[CrossRef](#)]
62. Zhang, L.; Liao, Y.; Tang, L. MicroRNA-34 family: A potential tumor suppressor and therapeutic candidate in cancer. *J. Exp. Clin. Cancer Res.* **2019**, *38*, 53. [[CrossRef](#)]
63. Edmonds, M.D.; Eischen, C.M. Differences in miRNA Expression in Early Stage Lung Adenocarcinomas that Did and Did Not Relapse. *PLoS ONE* **2014**, *9*, e101802. [[CrossRef](#)] [[PubMed](#)]
64. Yeh, C.-H.; Moles, R.; Nicot, C. Clinical significance of microRNAs in chronic and acute human leukemia. *Mol. Cancer* **2016**, *15*, 37. [[CrossRef](#)] [[PubMed](#)]
65. Agirre, X.; Vilas-Zornoza, A.; Jiménez-Velasco, A.; Martín-Subero, J.I.; Cordeu, L.; Gárate, L.; José-Eneriz, E.S.; Abizanda, G.; Rodríguez-Otero, P.; Fortes, P.; et al. Epigenetic silencing of the tumor suppressor microRNA Hsa-miR-124a regulates CDK6 expression and confers a poor prognosis in acute lymphoblastic leukemia. *Cancer Res.* **2009**, *69*, 4443–4453. [[CrossRef](#)]
66. Sugita, F.; Maki, K.; Nakamura, Y.; Sasaki, K.; Mitani, K. Overexpression of MIR9 indicates poor prognosis in acute lymphoblastic leukemia. *Leuk. Lymphoma* **2013**, *55*, 78–86. [[CrossRef](#)] [[PubMed](#)]
67. Liang, Y.-N.; Tang, Y.-L.; Ke, Z.-Y.; Chen, Y.-Q.; Luo, X.-Q.; Zhang, H.; Huang, L.-B. MiR-124 contributes to glucocorticoid resistance in acute lymphoblastic leukemia by promoting proliferation, inhibiting apoptosis and targeting the glucocorticoid receptor. *J. Steroid Biochem. Mol. Biol.* **2017**, *172*, 62–68. [[CrossRef](#)]
68. Oliveira, L.H.; Schiavinato, J.L.; Fráguas, M.S.; Lucena-Araujo, A.R.; Haddad, R.; Araújo, A.G.; Dalmazzo, L.F.; Rego, E.M.; Covas, D.T.; Zago, M.A.; et al. Potential roles of microRNA-29a in the molecular pathophysiology of T-cell acute lymphoblastic leukemia. *Cancer Sci.* **2015**, *106*, 1264–1277. [[CrossRef](#)]
69. Butrym, A.; Baczyńska, D.; Tukiendorf, A.; Rybka, J.; Dobosz, T.; Jurczak, W.; Kuliczkowski, K.; Mazur, G. High Expression of Mir-15a Predicts Shorter Survival and Worse Response to Chemotherapy in Patients with Acute Myeloid Leukemia (AML). *Blood* **2014**, *124*, 5330. [[CrossRef](#)]
70. Calin, G.; Croce, C.M. Chronic lymphocytic leukemia: Interplay between noncoding RNAs and protein-coding genes. *Blood* **2009**, *114*, 4761–4770. [[CrossRef](#)]
71. Qi, H.-X.; Cao, Q.; Sun, X.-Z.; Zhou, W.; Hong, Z.; Hu, J.; Juan, C.-X.; Li, S.; Kuai, W.-X. MiR-410 regulates malignant biological behavior of pediatric acute lymphoblastic leukemia through targeting FKBP5 and Akt signaling pathway. *Eur. Rev. Med. Pharmacol. Sci.* **2018**, *22*, 8797–8804.
72. Chirshv, E.; Oberg, K.C.; Ioffe, Y.J.; Unternaehrer, J.J. Let-7as biomarker, prognostic indicator, and therapy for precision medicine in cancer. *Clin. Transl. Med.* **2019**, *8*, 24. [[CrossRef](#)]
73. Huang, Y.; Hong, X.; Hu, J.; Lu, Q. Targeted regulation of miR-98 on E2F1 increases chemosensitivity of leukemia cells K562/A02. *OncoTargets Ther.* **2017**, *10*, 3233–3239. [[CrossRef](#)] [[PubMed](#)]
74. Horibata, S.; Gui, G.; Lack, J.; DeStefano, C.B.; Gottesman, M.M.; Hourigan, C.S. Heterogeneity in refractory acute myeloid leukemia. *Proc. Natl. Acad. Sci. USA* **2019**, *116*, 10494–10503. [[CrossRef](#)] [[PubMed](#)]

75. Qin, T.; Zhao, H.; Shao, Y.; Hu, N.; Shi, J.; Fu, L.; Zhang, Y. High expression of AK1 predicts inferior prognosis in acute myeloid leukemia patients undergoing chemotherapy. *Biosci. Rep.* **2020**, *40*, 1–10. [[CrossRef](#)] [[PubMed](#)]
76. Aly, R.M.; Ghazy, H.F. Prognostic significance of *MSI2* predicts unfavorable outcome in adult B-acute lymphoblastic leukemia. *Int. J. Lab. Hematol.* **2014**, *37*, 272–278. [[CrossRef](#)]
77. Zhao, H.Z.; Jia, M.; Luo, Z.B.; Cheng, Y.P.; Xu, X.J.; Zhang, J.Y.; Li, S.S.; Tang, Y.M. Prognostic significance of the Musashi-2 (*MSI2*) gene in childhood acute lymphoblastic leukemia. *Neoplasma* **2016**, *63*, 150–157. [[CrossRef](#)]
78. Schubert, C.; Allhoff, M.; Tillmann, S.; Maié, T.; Costa, I.G.; Lipka, D.B.; Schemionek, M.; Feldberg, K.; Baumeister, J.; Brümmendorf, T.H.; et al. Differential roles of STAT1 and STAT2 in the sensitivity of JAK2V617F- vs. BCR-ABL-positive cells to interferon alpha. *J. Hematol. Oncol.* **2019**, *12*, 36. [[CrossRef](#)]
79. Hodson, D.J.; Shaffer, A.L.; Xiao, W.; Wright, G.W.; Schmitz, R.; Phelan, J.D.; Yang, Y.; Webster, D.E.; Rui, L.; Kohlhammer, H.; et al. Regulation of normal B-cell differentiation and malignant B-cell survival by OCT2. *Proc. Natl. Acad. Sci. USA* **2016**, *113*, E2039–E2046. [[CrossRef](#)]
80. Advani, A.S.; Lim, K.; Gibson, S.; Shadman, M.; Jin, T.; Copelan, E.; Kalaycio, M.; Sekeres, M.A.; Sobecks, R.; Hsi, E. OCT-2 expression and OCT-2/BOB.1 co-expression predict prognosis in patients with newly diagnosed acute myeloid leukemia. *Leuk. Lymphoma* **2010**, *51*, 606–612. [[CrossRef](#)]
81. Sailo, B.L.; Banik, K.; Girisa, S.; Bordoloi, D.; Fan, L.; Halim, C.E.; Wang, H.; Kumar, A.P.; Zheng, D.; Mao, X.; et al. FBXW7 in Cancer: What Has Been Unraveled Thus Far? *Cancers* **2019**, *11*, 246. [[CrossRef](#)]
82. Franke, N.E.; Kaspers, G.L.; Assaraf, Y.G.; Van Meerloo, J.; Niewerth, D.; Kessler, F.L.; Poddighe, P.J.; Kole, J.; Smeets, S.J.; Ylstra, B.; et al. Exocytosis of polyubiquitinated proteins in bortezomib-resistant leukemia cells: A role for MARCKS in acquired resistance to proteasome inhibitors. *Oncotarget* **2016**, *7*, 74779–74796. [[CrossRef](#)]
83. Yang, Y.; Chen, Y.; Saha, M.N.; Chen, J.; Evans, K.; Qiu, L.; Reece, D.; Chen, G.; Chang, H. Targeting phospho-MARCKS overcomes drug-resistance and induces antitumor activity in preclinical models of multiple myeloma. *Leukemia* **2015**, *29*, 715–726. [[CrossRef](#)] [[PubMed](#)]
84. Lebedev, T.; Vagapova, E.; Popenko, V.I.; Leonova, O.G.; Spirin, P.V.; Prassolov, V.S. Two Receptors, Two Isoforms, Two Cancers: Comprehensive Analysis of KIT and TrkA Expression in Neuroblastoma and Acute Myeloid Leukemia. *Front. Oncol.* **2019**, *9*, 1046. [[CrossRef](#)] [[PubMed](#)]
85. Cloos, J.; Roeten, M.S.; Franke, N.E.; Van Meerloo, J.; Zweegman, S.; Kaspers, G.J.; Jansen, G. (Immuno)proteasomes as therapeutic target in acute leukemia. *Cancer Metastasis Rev.* **2017**, *36*, 599–615. [[CrossRef](#)] [[PubMed](#)]
86. Kang, H.; Wilson, C.S.; Harvey, R.C.; Chen, I.-M.; Murphy, M.H.; Atlas, S.R.; Bedrick, E.J.; Devidas, M.; Carroll, A.J.; Robinson, B.W.; et al. Gene expression profiles predictive of outcome and age in infant acute lymphoblastic leukemia: A Children’s Oncology Group study. *Blood* **2012**, *119*, 1872–1881. [[CrossRef](#)] [[PubMed](#)]
87. Wang, T.; Cheng, C.; Peng, L.; Gao, M.; Xi, M.; Rousseaux, S.; Khochbin, S.; Wang, J.; Mi, J. Combination of arsenic trioxide and Dasatinib: A new strategy to treat Philadelphia chromosome-positive acute lymphoblastic leukaemia. *J. Cell. Mol. Med.* **2017**, *22*, 1614–1626. [[CrossRef](#)]